©ISTOCKPHOTO.COM/IPOPBA

Soft Ultrathin Silicon Electronics for Soft Neural Interfaces

A review of recent advances of soft neural interfaces based on ultrathin silicon.

TECHNIQUES FOR CAPTURING electrical signals from the brain corresponding to most of the activities (actual or imagined) generated by neuron firing have provided neurologists with a fascinating path to decoding and studying this complex system. Technology to increase the spatiotemporal resolution of brain mapping tools has been advancing, aiming at highly dense electrode sites with the long-term stability of devices and negligible damage to brain tissue.

In this article, we discuss some of the recent advances in implantable soft silicon-based electronics devices that are devised for the long-term, minimally invasive, high-resolution recording of neural signals. We briefly introduce the different neural action-potential signals classified for different motor activities, and our review progresses through the advantages and acute requirements of developing

ANISH THUKRAL, FAHEEM ERSHAD, NADA ENAN, ZHOULYU RAO, AND CUNJIANG YU

Digital Object Identifier 10.1109/MNANO.2017.2781290
Date of publication: 17 January 2018

The brain is the most complicated of all processing units known, comprising billions of neurons and quadrillions of synapse connections.

high-resolution neural interface devices to promote progress in brain–machine interface (BMI) research. The requirements of high-density electrode coverage on the brain surface and the difficulty in achieving such density with the general design of neural interface devices that use passive electrodes are discussed. We also examine the recent advances in various neural devices with active electronic architectures, and the efficacy of silicon (Si) nanomembrane processing techniques in the construction of soft neural mapping tools.

TYPES OF NEURAL SIGNALS AND USES OF BMIs

The brain is the most complicated of all processing units known, comprising billions of neurons and quadrillions of synapse connections. Studying the brain, as the most complicated but most highly efficient system imaginable, has proven to be the greatest challenge for scientists and engineers in all fields striving to develop novel products, improve existing technology, and create computer interfaces to decode biological logic.

In the brain, neural signals called *action potentials* induce the flux of sodium and potassium ions through the neuronal membranes, which changes the concentration of ions in the extracellular fluid (ECF). The resting membrane potential of –60 mV increases to approximately 30 mV in such a depolarization event. The ion movement modifies the electrical potential in the ECF, and electroencephalography (EEG), electrocorticography (ECoG), and other recording methods can detect the changes in potential with respect to reference electrodes. The usual targets for neural recording are pyramidal cells, neurons whose cell bodies are 10–30 μm in diameter [1].

ECoG signals have low amplitudes (in the 10–500-μV range) and fall in the wide frequency range of 1–500 Hz. Five frequency bands are particularly important in research and clinical study.

1) Delta waves (1–4 Hz) are observed in dreamless sleep.
2) Theta waves (4–8 Hz) characterize dreaming or meditation states.
3) Alpha waves (8–12 Hz) are seen in the awake, resting state.
4) Beta waves (10–20 Hz) are apparent in attention-directing tasks. Brain-activity frequency bands in the range of 8–12 Hz and 18–25 Hz are important for BMI systems, as they contain information about imagined movement [2], [3].
5) Higher-frequency bands, such as those above 60 Hz (high gamma bands), show awake, sensorimotor activity and processing of information from multiple brain regions, and are of great interest to researchers [4].

Changes in the broadband gamma range indicate the firing rates of neurons directly below the recording electrodes and are unique to specific tasks [5]–[7]. The high gamma band is particularly important, because it correlates with neural firing and contains a rich representation of biological signals, i.e., it reveals the motor kinematics of a living being [8]. It is difficult to obtain these signals from EEG [9]. Also, commonly observed frequencies in moderate anesthetic states are in the delta band (1–4 Hz) and theta band (4–8 Hz) [4]. Figure 1(a) shows the brain sections for action potentials corresponding to different neural activities.

Various neurological diseases can hinder a patient's motor function, making it enormously difficult to lead a self-sufficient life. But with BMIs, ECoG can be utilized to record action potentials from target areas of the brain and decode the signals by interfacing them with high-end computers to control various machines. The application of advanced BMI systems can be extended to the well-controlled movements of prosthetic limbs maneuvered by a person's thoughts. Typically, the individual using such a system lives with a broken motor pathway that interrupts communication between muscles and the nervous system [10]. BMIs provide a direct communication pathway between the brain and a machine. Some examples include the neural control of a robotic arm by using just thoughts or the manipulation of a computer cursor and its related communication program in the same way [11], [12]. BMIs have four primary functions:

1) recording neural activity
2) interpreting neural activity as an intended action
3) controlling a device that performs the action
4) providing feedback to the subject.

In other words, BMIs can take imagined movements and turn them into actual ones by recording action potentials from the cortical surface and decoding them. Hence, BMIs have significant potential to improve the quality of life for those with neurological disorders. These devices' higher spatial resolution and specificity allow for greater accuracy in BMI research [13]. Figure 1(b) represents a typical flowchart for a BMI system.

In addition to the application to action-potential recordings, neural stimulation is a promising technology for the treatment of severe neurological dysfunction. Deep-penetrating optoelectronics have been used for triggering or stimulating light-sensitive components in the brain. Moreover, optogenetic intervention has been used to illuminate the brain's neural connectivity and circuitry. By transfecting specific types of neurons with deoxyribonucleic acid that encodes for opsins, or proteins that change their conformation in response to light, spatiotemporal control of the activation and inhibition of neural activity has been achieved [14], [15]. This sort of cell-type specificity in neuromodulation cannot be realized with simple electrical stimulation, as the latter causes a

membrane depolarization of not only the target neurons but the nearby neurons in a brain region [16].

Fiber-optic light is the traditional light-delivery method, but there have been developments in inorganic light-emitting diodes (LEDs) and μLEDs [17], [18]. LEDs replace the need for inserting the often-used silica waveguide. At the same time, soft, biocompatible, and mechanically compliant materials are required to investigate deeper brain structures to circumvent various issues, e.g., glial scar formation, that occur with inserting conventional recording technologies and fiber-optic devices.

EXISTING NEURAL INTERFACE TECHNOLOGIES

EEG is the simplest and most commonly used method for capturing neural signals. Although it is safe, it requires the subject to wear a nonergonomic helmet on top of the head that requires regular repositioning and recalibration. Relatively softer and flexible ECoG devices provide safe interface during operation, designed with purpose of minimum damage to subdural meninges and cortical tissue [19]. This technique is less sensitive to artifacts, offers higher frequency and spatial resolution, can better obtain continuously accurate localizations [20], and has a more robust signal-to-noise ratio (SNR) than EEG.

Microelectrodes, which are also referred to as *neural probes* or *tissue-penetrating electrodes*, are a more specific option than ECoG in terms of frequency and spatial resolution. However, long-term robustness is still an issue, and potential side effects hinder the practicality of this recording modality [21]. Tissue-penetrating electrode arrays (with an electrode diameter of 40 μm and 0.4–1-mm spacing) have shown that epileptiform activity can be localized to the submillimeter scale. Penetrating microelectrodes have been shown to achieve micron-scale spatial resolution. However, these electrodes can damage surrounding tissue and are commonly used in a resection area. They fail to define the boundaries of the epileptic activity, and this also holds true for mapping the motor or language cortex [22]. EEG signal quality is not sufficient for a wide range of BMI applications [23]. ECoG has the potential to produce stable, long-term recordings compared to action-potential recordings, since ECoG implants do not pierce the cortex.

There are other neural recording or imaging modalities that are frequently compared to ECoG. Functional magnetic resonance imaging (fMRI) is a mapping technique known for its non-invasive application and high spatial resolution [24]. It is used to measure

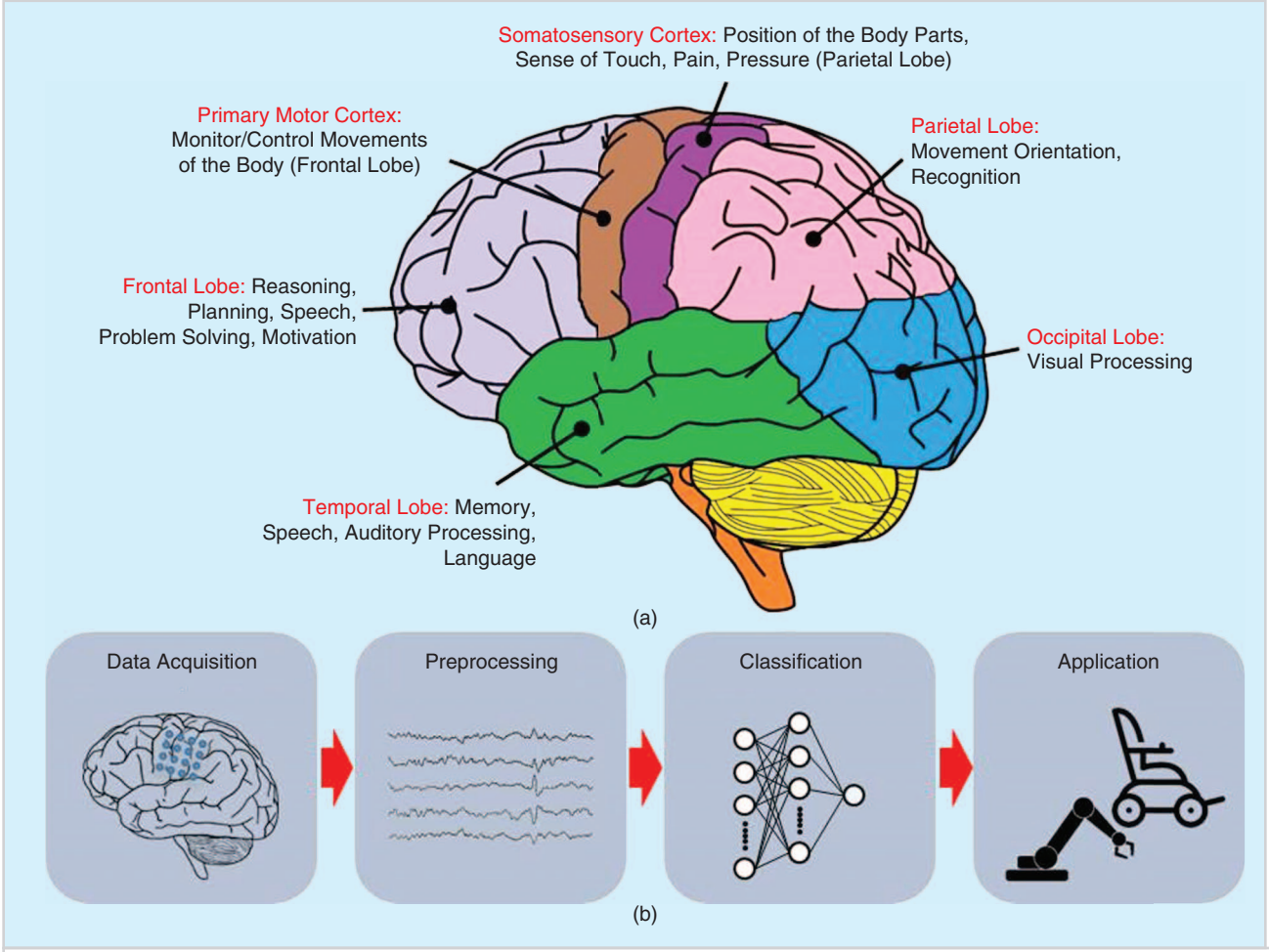

FIGURE 1 (a) The parts of the brain that correspond to various neural activities. (b) A BMI system flowchart.

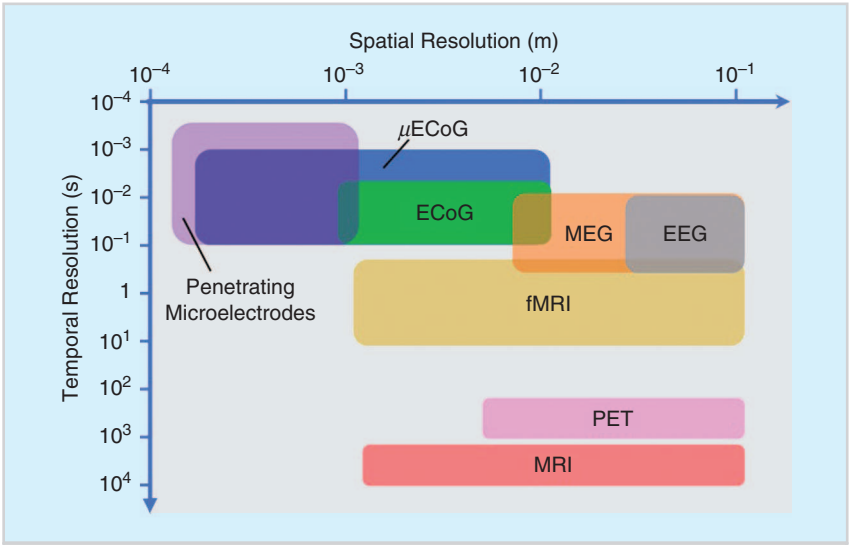

FIGURE 2 The various neural recording and imaging techniques, comparing their temporal and spatial resolution.

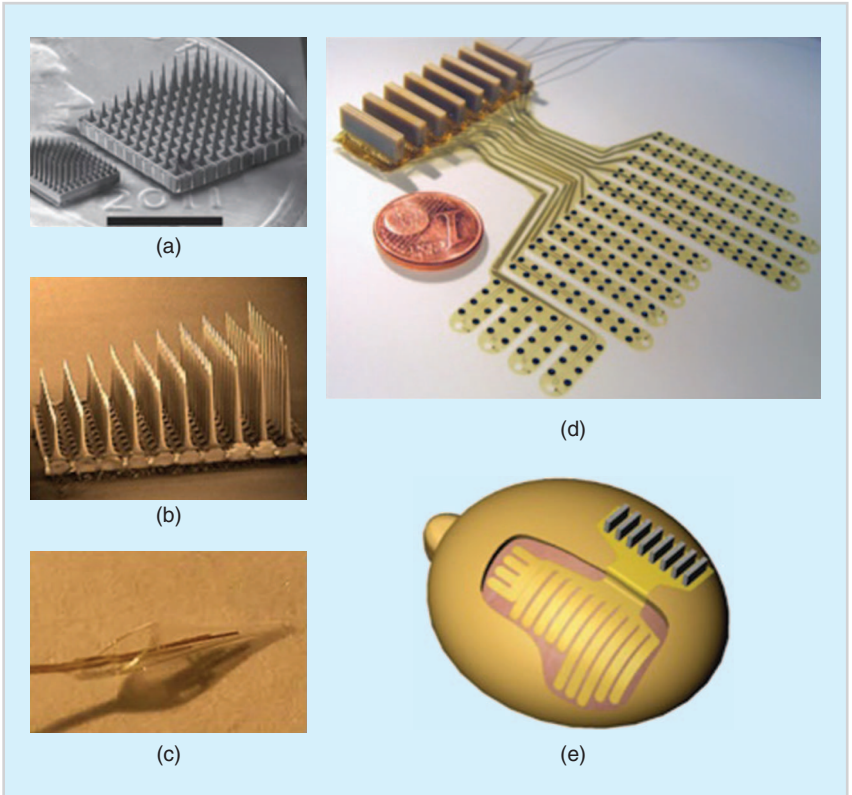

FIGURE 3 (a) and (b) A typical neural probe electrode array [28], [29], (c) a cone electrode [30], (d) an ECoG array with bulky connectors, and (e) the same array shown implanted on the surface of the brain [47].

neural activity through observing the changes in blood-oxygen-level-dependent (BOLD) signals [25]. The main drawback of this method is that it offers an indirect evaluation of neuronal activity by just imaging the contrast of blood oxygen levels of active areas of the brain during a task [24].

However, ECoG recordings have been found to correlate with fMRI BOLD signals. ECoG's spatial resolution, which ranges from the millimeter scale to a few centimeters, is relatively similar compared to that of other neural recording and neuroimaging methods, such as fMRI, positron emission tomography (PET), and MRI [26], as shown in Figure 2. But ECoG has a much higher temporal resolution than fMRI, PET, and MRI, as ECoG ranges from 5 ms to approximately 0.1 s [27], while the others are from a few seconds (fMRI) to minutes (PET) or even hours (MRI). ECoG is commonly compared to EEG and magnetoencephalography (MEG), both of which overlap in spatial and temporal resolution (10 mm–10 cm and 10 ms–1 s, respectively) but, clearly, intervention of electronic design and fabrication technology is pushing the ECoGs toward much higher spatial resolution, as shown in Figure 2.

Hence, electrophysiological techniques are of great significance for advancing BMI technology, where ECoG represents the optimum technique over EEG and neural probes. ECoG is superior to EEG because direct recordings from the brain are less susceptible to signal distortion and user movements; as with EEG, the signals must travel through the different muscle layers and the passive skull. Furthermore, ECoG surpasses neural probes because the ECoG patch that rests on the surface of the brain allows for long-term operation, with higher area coverage and safer recordings, engendering fewer health issues than the neural probe electrodes that penetrate into the brain tissue. The devices generally used for neural recordings (through neural probes) are mostly Si-based mechanisms—sharp microneedles—that penetrate deep into the brain tissue [28], [29]. A typical electrode array is shown in Figure 3(a) and (b). Another famous and commonly used device is the cone electrode in Figure 3(c) [30].

SOFT ELECTRONICS FOR NEURAL MAPPING

DEVICE STRUCTURE FOR NEURAL MAPPING

Because of the acceptably low invasiveness of the technique, ECoG is one of the most promising tools for neuroscientists and neural engineers to observe brain activity. The ECoG device utilizes the separation between two conductors to sense a differential potential between

two sites, with each site consisting of a batch of neurons beneath. The action potential generated at a specific site is measured as a differential with the other site. The clinical ECoG device that developed over time comprises multiple electrodes on a substrate to form a patch directly implanted on a cortical site.

Direct contact of the electrodes with the brain surface creates a critical need to understand the interaction of the two surfaces. Brain tissues are extremely soft, with a stiffness to the order of 100 Pa [31]. In interfacing with such soft materials, a profound insight into the mechanical mismatch of the interacting tools is necessary. Elastic mismatch and material density mismatch [32], [33] can cause severe damage to brain tissues, including glial scarring or infarction [34] and vascular damage, even with micromovements. Similarly, exceedingly stiff Si neural probes (the Michigan probe and Utah array) that are routinely used cause the neuroimmune system to resist the poking or insertion of external abiotic bodies, activating a foreign-body response and causing neural inflammation. Therefore, this section reviews some of the crucial requirements for the mechanical properties of a cortical implant.

For both short- and long-term measurements, the device should possess certain physical properties. The materials of which it is made demand high biocompatibility to avoid toxicity in the biological system, and they must be nonreactive with biofluids. The brain anatomy is intricate and comprises a curvilinear surface characterized by wrinkles (surface roughness), grooves (sulci), and bumps (blood vessels). The conformal contact with the brain surface is another crucial factor to consider. To precisely capture brain signals, there needs to be proper electrical contact between the electrode and the cortical surface. The irregularities on the brain surface tend to loosen the contact with the electrodes, which engenders a significant increase in electrode impedance. Improper connections can lead to an increase in impedance because of the increase in capacitance between the device and the cortical surface. To meet the necessary requirements, the device should be capable of making conformal contact with the irregular curvilinear

The materials of which a brain implant is made demand high biocompatibility to avoid toxicity in the biological system.

profile of the brain. Yet even after extensive development, ECoG devices are bulky patches that can cause significant elastic mismatch with the brain surface and, hence, lack the important requirements just described. The effective solution to the mechanical compatibility of these devices lies in thin-film engineering.

The mechanical bending stiffness or the bending moment of inertia of a structure is directly proportional to the cubic power of the thickness of a structure. Therefore, reducing the thickness of a film can significantly minimize the bending stiffness and make the structure highly compliant. S. Wang et al. [35] found that, for conformal contact with a microintricate surface, the thickness of the structure needs to decrease to a few microns to reduce the total energy, known as the *conformal energy*, which is the sum of the bending energy, the elastic energy of the rough surface (skin), and the interfacial adhesion energy. Furthermore, mechanical imperceptibility is as critical as conformal contact, so an ultrathin device structure is, again, at an advantage over its bulky counterpart. Figure 4 demonstrates the conformal contact of a thin film on a typical curvilinear model of the skin surface.

A study of the surface conformability of thin-film ECoG by D.-H. Kim et al. [36] further revealed the accuracy of Wang et al.'s computations by computing a device thickness of less than 4.9 μm for conformal contact with the brain surface model. The results showed that not only thinness but an open mesh structure (rather than a thin continuous film) was an advantage for conformal contact because of the comparatively lower adhesion energy required by the mesh structure design than the corresponding sheet design. As shown in Figure 5, the device 2.5-μm thick has better contact with the

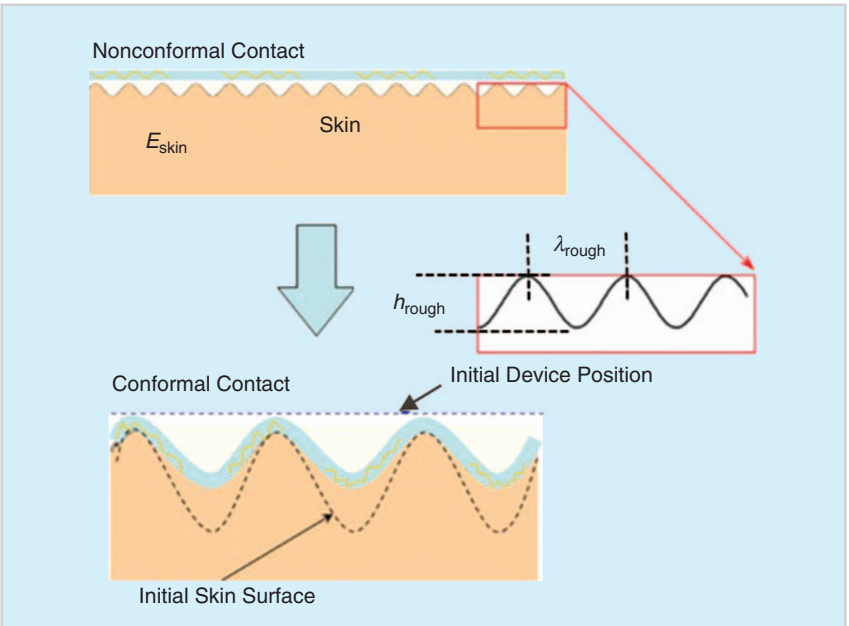

FIGURE 4 The conformal contact of a thin film on a curvilinear skin surface [35].

brain surface than the one with a thickness of 76 μm, which is further improved by a mesh structure 2.5-μm thick. Moreover, the authors claimed that in addition to the relatively higher adhesion energy required by the sheet structure, relatively higher membrane strains in the sheet design of similar thickness than the mesh design caused comparatively high wrinkles in the sheet that reduced conformability. In contrast, the mesh structure, having significantly high stability over wrinkling, allocates any possible wrinkles in the open spaces (holes) of the mesh and, hence, avoids nonconformability due to wrinkles. The data map also revealed a direct correlation between the effectiveness of ECoG devices and their conformability, where signals are more effectively received with the 2.5-μm mesh structure than with the 2.5-μm sheet device, and much better than with the thick film.

The substrate material also plays a significant role in surface adhesion. As the brain contains biofluid, the hydrophilic nature of the substrate material is important for a film's adhesion to the brain surface during any relative movements in the brain or pulsations due to blood flow. Besides the mechanics of reducing bending stiffness, there have been alternative methods proposed to achieve a significant conformability of electronic devices. Other approaches to increasing device conformability are creating strain-allocated designs through strain engineering [37]–[39] and utilizing adhesive gels [40].

HIGH-DENSITY MAPPING

The electrodes mesh is the sole working member in ECoG in the terms of collecting signals or stimulating neural activities in the brain. The location of the electrodes thus directly influences the signals that are received from the brain and interfaced with the computer. Clinical ECoG devices generally have an array of electrodes ranging from 3 × 3 to 16 × 16 arrangements, with an electrode diameter of 2–3 mm and an interelectrode pitch of 2–4 cm. These clinical electrodes can realize action-potential signals from the brain for a general understanding of well-being, but they are not sufficient for the detailed analysis of various neural problems, for the study of root causes of severe neural diseases, and to interface with machines for advanced neurally controlled prostheses. Such coarsely dense electrodes are not adequate for the precise mapping of the wide range of motor activities, which is a critical requirement for advanced BMIs. What is needed is the ability to decode neural signals for accurately specifying and differentiating the wide range of control activities in novel BMI applications. Also required is the capacity to precisely map highly spatiotemporally resolved neurons covering a broad area of the brain to capture more localized variations in action potentials.

A study by X. Wang et al. [41] found the response peaks to be fewer than 1 cm apart, which is a more localized region than that found with the typical interelectrode pitch in an ECoG device. Therefore, to accomplish a precise, localized mapping of action potentials, the ECoG implant requires much higher spatial resolution. In other words, progress in BMI applications requires the development of a highly dense array of electrodes to precisely process action potentials. The advent of microfabrication techniques provides hope for realizing such dense-electrode devices.

Recent studies show the efficacy of this approach of utilizing high-density ECoG electrode arrays in advancing BMI performance. P.T. Wang et al. [42] demonstrated the precision of high-density ECoG electrodes in controlling the movement of a prosthetic arm with six degrees of freedom. The researchers proved the efficacy of dense ECoG electrodes versus the clinically available low-spatial-resolution electrodes.

Several reports have investigated the size and interelectrode distance of ECoG electrodes [43], [44]. For a fixed brain area to be covered, increasing the electrode density by decreasing the interelectrode pitch (from a few centimeters to a scale of millimeters or micrometers) and reducing the size of the electrodes (from

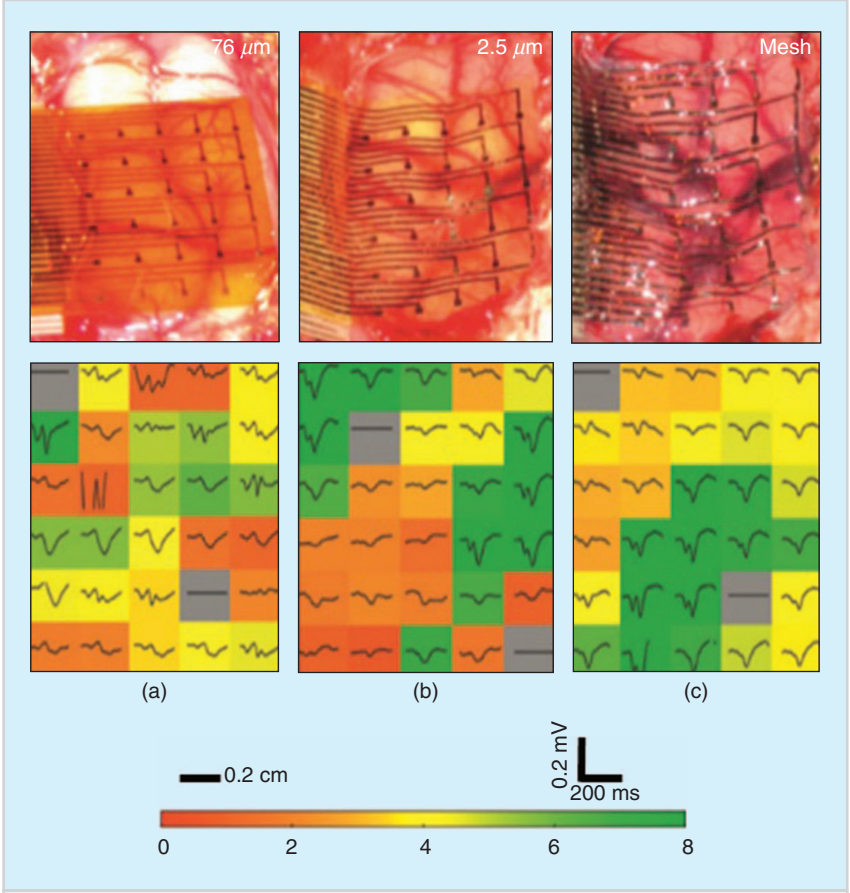

FIGURE 5 The cortical conformability of ECoG devices that are (a) a 76-μm-thick continuous film, (b) a 2.5-μm-thick continuous film, and (c) a 2.5-μm-thick mesh film [36].

millimeters to micrometers) enabled the capture of brain activities at a higher spatial resolution, which resulted in a larger and more comprehensive data set. Neural and electrical engineers have already achieved a microsize electrode diameter and have termed the devices as μECoG.

Techniques based on μECoG were academically accepted and studied by various research groups, demonstrating an improvement in spatiotemporal resolution. For example, W. Wang et al. [45] demonstrated the improvement in a μECoG BMI in terms of the movement of a prosthetic arm and fingers.

Although there have been multiple studies advancing BMI applications via improvements in spatiotemporal resolution using highly dense electrode arrays, there are also a number of disadvantages associated with high-density electrode meshing in terms of capturing action potentials. A reduction in the size of an electrode limits its contact area with the brain surface, which increases its impedance in capturing the cortical signal and reduces the SNR. Most μECoG studies involved high-frequency signal detection. But reducing the interelectrode gap (pitch) can sacrifice the spatiotemporal resolution of low-frequency signals by increasing their correlation and coherence [46], making them indistinguishable. Besides sacrificing this resolution, it is challenging to wire all of the electrodes to the output processing circuit. Birthe et al. [47] designed a device with 252 channels in a polyimide substrate to cover a wide area of the brain surface, but, as shown in Figure 3(d) and (e), it is challenging and not advisable to use such bulky connectors on a person's skull, especially when the user is performing routine activities and is not under the influence of anesthetics.

ULTRATHIN Si-BASED SOFT NEURAL PROBES

To utilize and advance novel BMI applications, it is crucial to solve all of the existing problems and aforementioned limitations. The engineering solution lies in designing and using soft devices that have significantly low bending stiffness to reduce the mechanical mismatch and in utilizing active-circuit technology to achieve high-density electrodes for increasing spatiotemporal resolution. This section will discuss the progress made in soft neural implants.

The engineering solution lies in designing and using soft devices that have significantly low bending stiffness.

Most of the recent studies that have advanced the state of the art in neural device implants have approached their work on the basis of reducing the mechanical mismatch between the soft brain tissue and the stiff substrate of existing neural implants. Xiang and colleagues [48], inspired by the design and measurement efficiency of the stiff Si needles of the Utah microelectrode array, developed a relatively softer array using an ultrathin polyimide substrate and SU-8 microneedles, as shown in Figure 6(c). The ultrathin, mesh-structured polyimide functions as a highly conformal substrate, while the SU-8 provides the softness required for the neural probes. The 40–200-μm-diameter needles are coated with a thin gold film to act as electrodes that impinge into the brain tissue.

Although the noted leading-edge devices are significantly improved in softness, thick probes can cause tissue damage through micromovements, dimples, and infarctions in the brain tissue during insertion or retraction. To address this, engineers have tried the novel approach of mechanically tuning the devices upon implantation. Shen et al. [49] utilized collagen, a highly biocompatible material, to act as a mechanically strong support for the easy insertion of a device into intracranial tissues. The authors utilized the collagen's mechanical property to become soft on hydrolysis during insertion. Utilizing the extracellular matrix (ECM) protein as a possible substrate for appreciable material and mechanical compatibility with the brain intracellular environment could possibly reduce the issue of any foreign-body immune response and mechanical infarction of the tissues during implantation, removal, or when under micromotion. Figure 6(e) introduces the detailed schematic steps of the fabrication of an ECM-supported neural probe.

Along with neural probes, Rogers and coworkers [17] took ultrathin intracranial implants to the next level by affixing functional optoelectronic and electronic devices on an ultrathin substrate to create soft, mechanically compliant devices for the study of brain signals. Figure 6(a) presents the multilayer, thin-film semiconductor, micromembrane material-based, multifunctional implantable device. These contrivances consist of μLEDs, microscale Si membrane-based photodetectors, milli-Kelvin precise temperature sensors/microheaters, and platinum (Pt) microelectrodes for neural recordings and electrical stimulation. They are 20 μm in thickness, which is a tenth as thin as the softer microneedles discussed earlier—exceptionally thin for such multidevice neural implants. The low bending stiffness and appreciable flexibility make the devices highly suitable for long-term semiinvasive use in deep-injectable neural devices, possibly entailing minimal mechanical damage to the brain tissue on surgical injection and retraction or with micromotions. Hence, there is promise that they will become an exceptionally advanced future tool for optogenetics and other neural-interface applications.

Recently, our group developed soft penetrating probes based on ultrathin Si based optoelectronic devices for future implementation in BMI [59]. Utilizing an ultrathin polyimide substrate for mechanically compliant and curvilinear conformability, the team fabricated single-crystal p-Si and n-Si n–p diodes in n–p–p–n-configured photodetector devices employing the typical transfer process after releasing the doped and patterned Si photodetectors from atop a silicon dioxide (SiO_2) layer using a buffered oxide etchant.

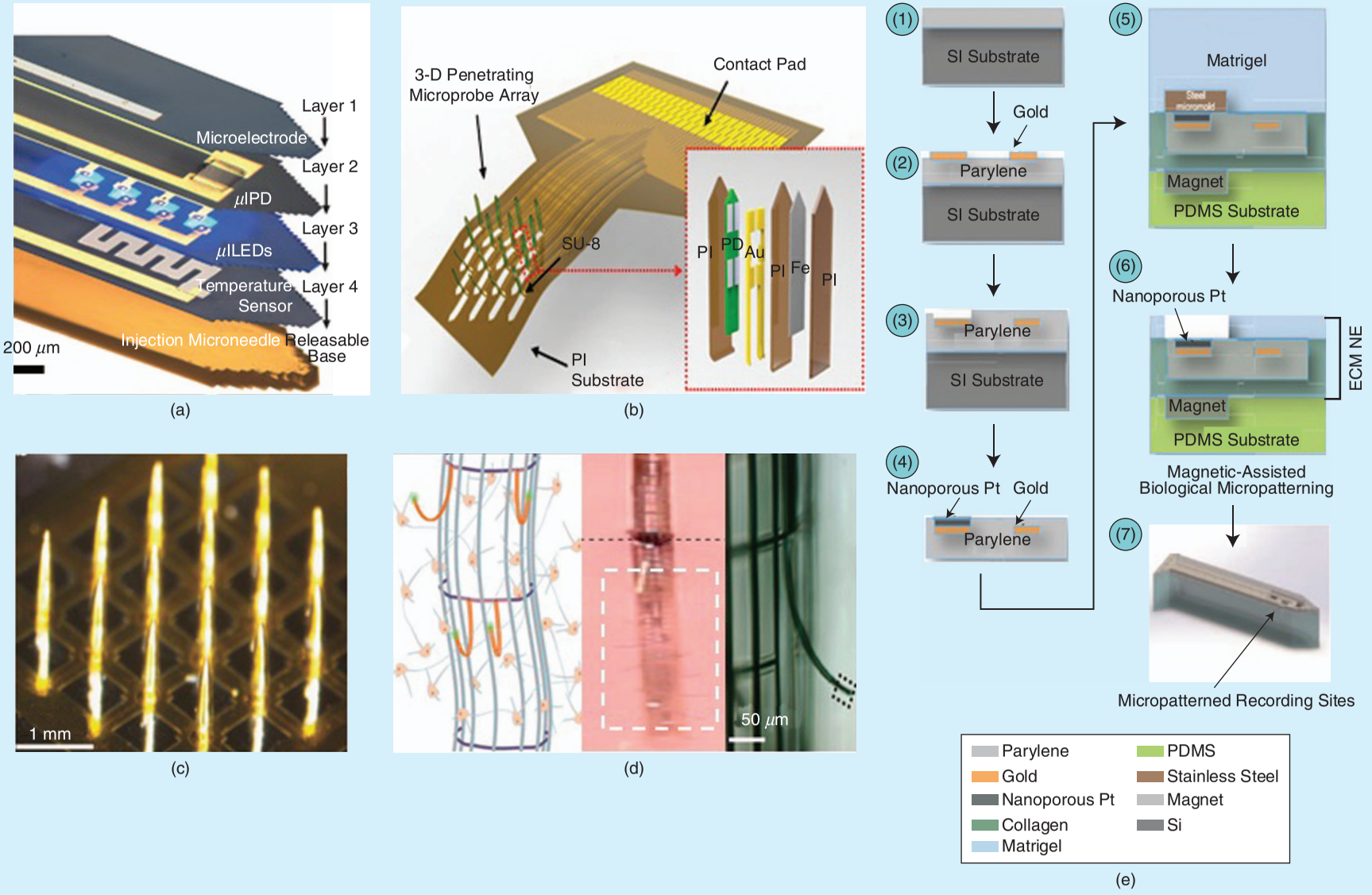

FIGURE 6 (a) A multilayer thin-film neural implantable device [17]. (b) An ultrathin, soft Si membrane-based microelectrode array for deep neural implants [59]. (c) A close-up of the soft microprobe array [48]. (d) The external curved surface of the cylindrical mesh of the neural probe contains electronic sensors and/or Si nanowire-based transistors reference [51]. (e) The detailed schematic steps in creating an ECM-supported neural probe [49]. PDMS: polydimethylsiloxane; μPD: microphotodetector; PI: polyimide; PD: photodetector; Au: gold; Fe: iron.

Figure 6(b) represents the ultrathin, soft Si membrane-based microelectrode array for deep neural implants. Such soft Si-based microelectrode array contrivances demonstrate promising progress in neural implants toward achieving mechanisms for short- and long-term measurement in neural engineering. Several other significant research works have been published in the related field of ultrathin soft neural electrodes [50], [51] that utilize the softness of the penetrating devices for negligible tissue damage in long-term use of the devices.

ULTRATHIN Si-CIRCUIT-BASED SOFT ECoGs

Electrical circuit physics is comprised of two categories of components: passive and active. The active elements modulate the actual signals and make them easily processable. Semiconductor device technology has, to a great extent, been developed to be implemented in electronic circuits. Most of the conductive electrodes in an ECoG array are nothing but metal connections that transfer the charge to externally generate the voltage peaks; i.e., the electrodes are passive. The signals can be processed by implementing active devices to modulate the action potentials to amplify the signals [52] for higher SNR or by using matrix multiplexing circuit technology [53] to simplify the wiring connections by using switches and reducing output lines. Hence, using active-device-circuit architecture, most of the aforementioned problems can be solved.

Rogers and coworkers also [54] combined active-circuit components comprising Si as the active component material and high-mobility Si transistors as switches and buffer components to design a matrix multiplexing architecture to realize significantly dense ECoG electrodes on an extremely thin polyimide film substrate. The device was the first of its kind to utilize active-circuit architecture for thin-film μECoG technology. Besides the circuit architecture, the active material processing and the device fabrication itself proved to be beneficial in the development of a novel neural engineering technology. The article discussed the development of a soft μECoG device with a high density of electrodes to achieve high spatiotemporal resolution—a neural interface that opens wider possibilities for next-generation BMI technology. Its soft nature promises safer tribology at the device–brain interface, and its microscale thickness provides high bending stability and significantly small bending strain on all the active materials in the device, compared to their respective fracture limits.

Figure 7(a) shows a typical architecture for a single electrode in Rogers et al.'s device, where each Pt electrode for capturing action potentials was integrated with a buffer Si-based transistor and the same Si transistor-based switch. The transistor was combined with the electrode to provide buffering of the action potential from the brain, and the second transistor was the multiplexing switch that combined all of the electrodes in a column to be operated with one connecting output wire. Figure 7(b) presents the performance of a typical Si membrane transistor that was integrated in the multiplexing system of the soft μECoG device. Figure 7(c) reveals the bending stiffness modulation by varying the thickness of the substrate and, hence, the overall device thickness. The high bending stability allows the device to fold and demonstrates the application of thin-film μECoG electrodes on the brain by conforming with even small intricacies and capturing signals from sulci regions as well. Figure 7(e) shows the implementation of a foldable, thin-film, high-density μECoG device.

Lieber and coworkers [51] fabricated Si nanowire-based ultrathin neural probes to detect single-unit action potentials from the deep brain. The device's ultrathin design, macroporous mesh, and cylindrical curvature made it the first of its unique type of neural probe. The external curved surface of the cylindrical mesh contains electronic sensors and/or Si nanowire-based transistors, as shown in Figure 6(d). Clearly mentioned in [51] is that, by reducing the thickness and providing a highly porous structure (80% porosity), the device's bending stiffness became four-to-seven orders of magnitude less than existing Si-based stiff neural probes [shown in Figure 3(a) and (b)]. This provided the sensor arrays with the cellular-level compliancy that was confirmed by the calculated deflection force of 1 nN/μm. The device demonstrated an excellent utilization of macropores to reduce the accumulation of neurons around the probe, which is a typical problem in almost all neural probes, including cone-shaped ones [shown in Figure 3(c)]. Multiplexing the electrodes or electronic sensors around the cylindrical body also widens the scope of the brilliant idea of using macroporous ultrathin-film neural probes with active-circuit components. Porosity, however, limits high-density measurement along the length of the probe.

Similar technology integrating active-circuit components with devices to capture high-resolution electronic imaging from cellular bionic sources is being developed by other research groups [55], [56] utilizing analogous approaches. However, we limit our review to soft neural devices based on Si nanomembranes.

Microfabrication technology has significantly progressed toward reducing bulky electromechanical systems to the microscale. Numerous such technologies have been well developed to realize thin-film Si-based electronics, including solution-based thin-film processing [57], although it is limited by the relatively lower mobility of amorphous or p-crystalline Si material. Manufacturing high-mobility, single-crystal Si-based soft devices utilizes a typical technique of transfer-printing the Si nanomembrane and multilayer processing. The commonly used Si nanomembrane transfer printing process—in which highly doped 250-nm-thick Si nanoribbons are printed to a polyimide substrate—is sequentially described in Figure 8 from the aforementioned article [54]. The electrodes were deposited, followed by polyimide encapsulation, and finally deposition of Pt electrodes. The encapsulation layer prevents leakage from the highly conductive biofluid.

Bioresorbability is the next important advance in noninvasive implantable electronic devices. Particularly in the case of brain implants, two key surgical steps are involved in implanting and removing the device after its operation is no longer needed. Experiments for neural studies and possibly existing or novel applications for BMIs target the capture of neural signals over a longer duration. For instance, to provide a paralytic with prosthetics that

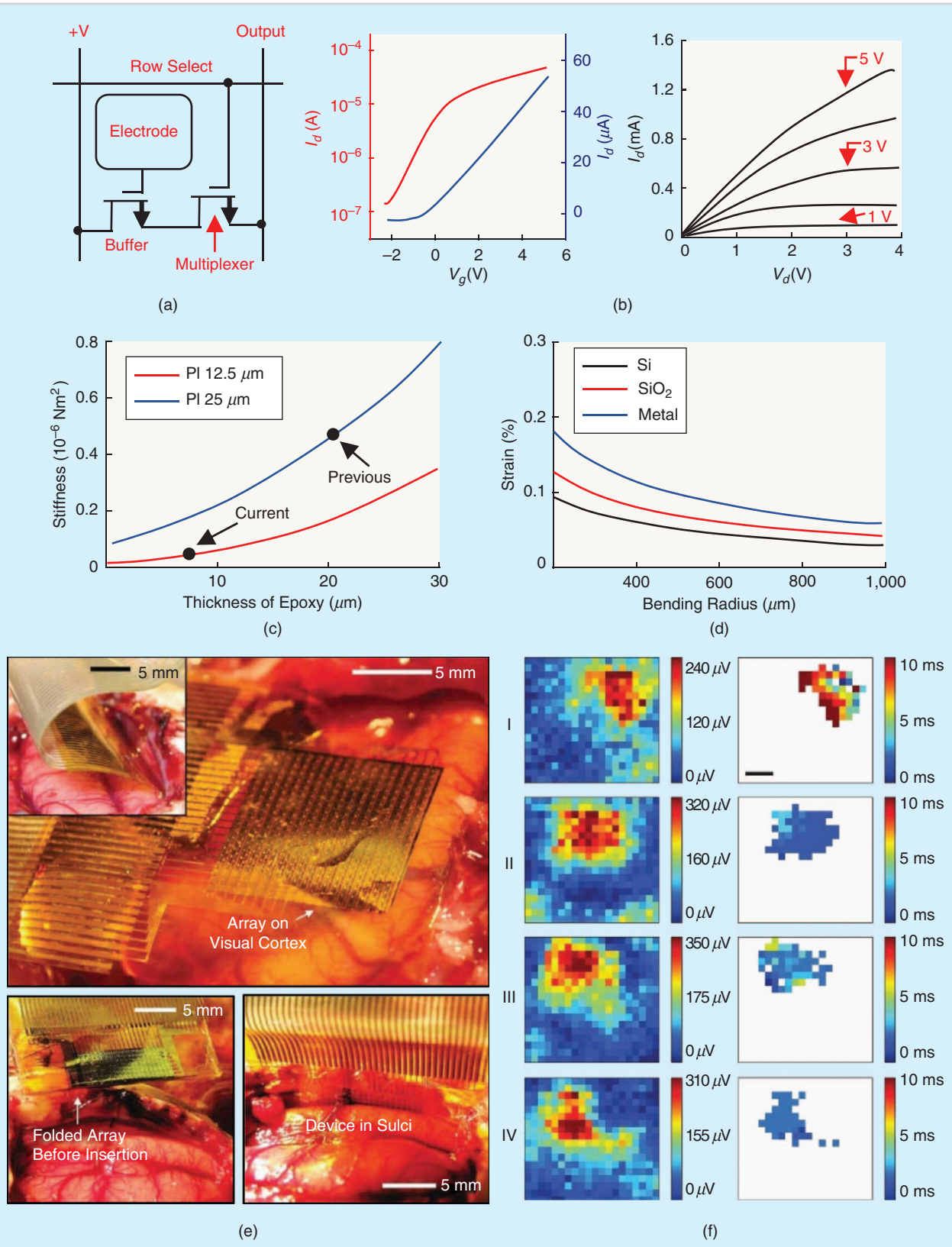

FIGURE 7 (a) The typical architecture of a single electrode in the multiplexed device. (b) The performance of a typical Si membrane transistor that was integrated in the multiplexing system of the soft μECoG device. (c) The bending stiffness of the device as it varies with the thickness of the substrate. (d) An indication of the device's high bending stability. (e) The implementation of the foldable, thin-film, high-density μECoG device. (f) Highly spatiotemporal resolved neural mapping corresponding to sleeping spindles from the brain using the active ECoG [54].

can be directly controlled by the individual's thought through the BMI requires that the person keep the ECoG device for a longer period of time. To implant and remove the ECoG hardware, the person needs to be treated and monitored in an intensive-care unit while all of the physiological conditions required to maintain critical human body operations are controlled. This is especially true when intracranial body parts are exposed; conditions need to be well maintained to prevent seizures. Operations, then, are always time consuming and costly, and there is always a need to find solutions that avoid surgery.

Rogers and coworkers [54] developed and demonstrated an Si nanomembrane-based, highly dense μECoG device capable of slowly dissolving over time. They achieved such a device by using resorbable materials [Figure 9(a)] in the electrodes for capturing the action potentials, in the material for the active-circuit devices [Figure 9(f) and (g)], and in the substrate. All of these materials should be capable of dissolving in the biofluids, and the final products should be biocompatible with and nontoxic to a subject's body. The report discussed utilizing a highly p-doped 300-nm-thick Si nanomembrane as the active component material, 100-nm-thick SiO_2 as the dielectric layer and as the isolation layer from the tissues and highly conductive biofluids, and 30-μm-thick poly(lactic-coglycolic acid) polymer as the biodegradable thin-film substrate, shown as a schematic in Figure 9(d).

Instead of using Pt for their signal-capturing electrodes as they did in their previous report, here, the team used highly doped p-type Si as the electrode material. With the 250- × 250-μm^2 dimensions of its exposed electrodes, the device was a μECoG device. Combining the passive and active components using biocompatible and nontoxic materials as shown in schematic Figure 9(d) opens the possibility of a bioresorbable device that can achieve high spatiotemporal resolution. Hence, employing a nanoscale-thick membrane of intrinsically stiff Si enormously reduces the bending stiffness, making it compatible with the soft nature of the implantable electronics. Utilization of the previously discussed active-device matrix multiplexing circuit architecture

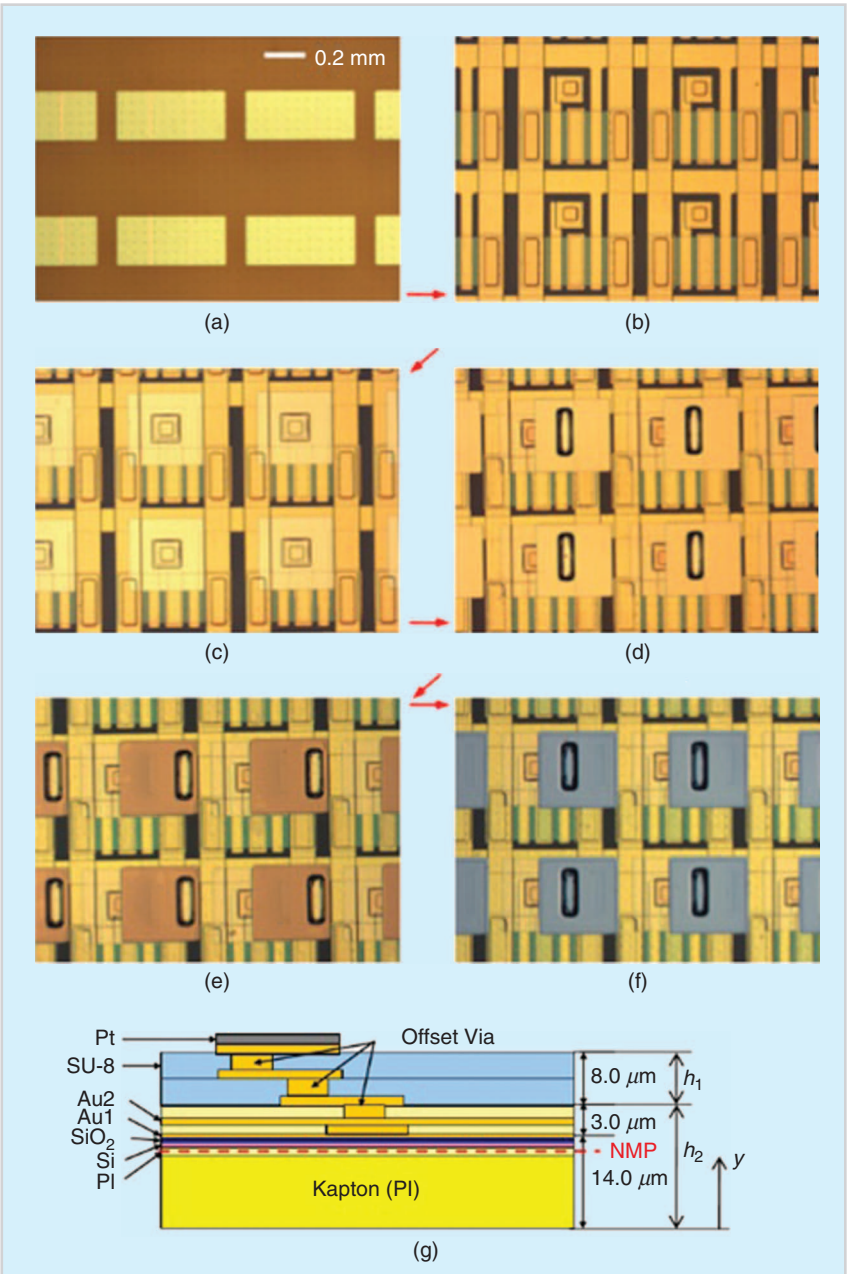

FIGURE 8 The commonly used Si nanomembrane transfer printing process: (a) the doped Si nanoribbons, (b) the first and second interconnects, (c) the third metal for contact electrode, (d) the fourth metal after the first epoxy encapsulation, (e) the fifth metal after the second epoxy encapsulation, (f) the final Pt deposition, and (g) a cross-section view of the final result [54]. NMP: neutral mechanical plane.

can help this approach to achieve high spatiotemporal resolution. Deploying the mechanism of bioresorbable nontoxic materials for long-term use of the μECoG device on an active person to capture action potentials from the user's regular day activities creates the promise of significant advances in BMIs in the near future.

Furthermore, it is important to mention that the kinematics of the bioresorbable device is a vital parameter. The report showed that the device's mechanism was a slow but continuous process that dissolved the Si and SiO_2 materials into neutral orthosilicic acid. The reaction rate strongly depended upon the pH level of the surrounding environment, the temperature, and even the impurity level of the Si material. As the device needs to operate for a long

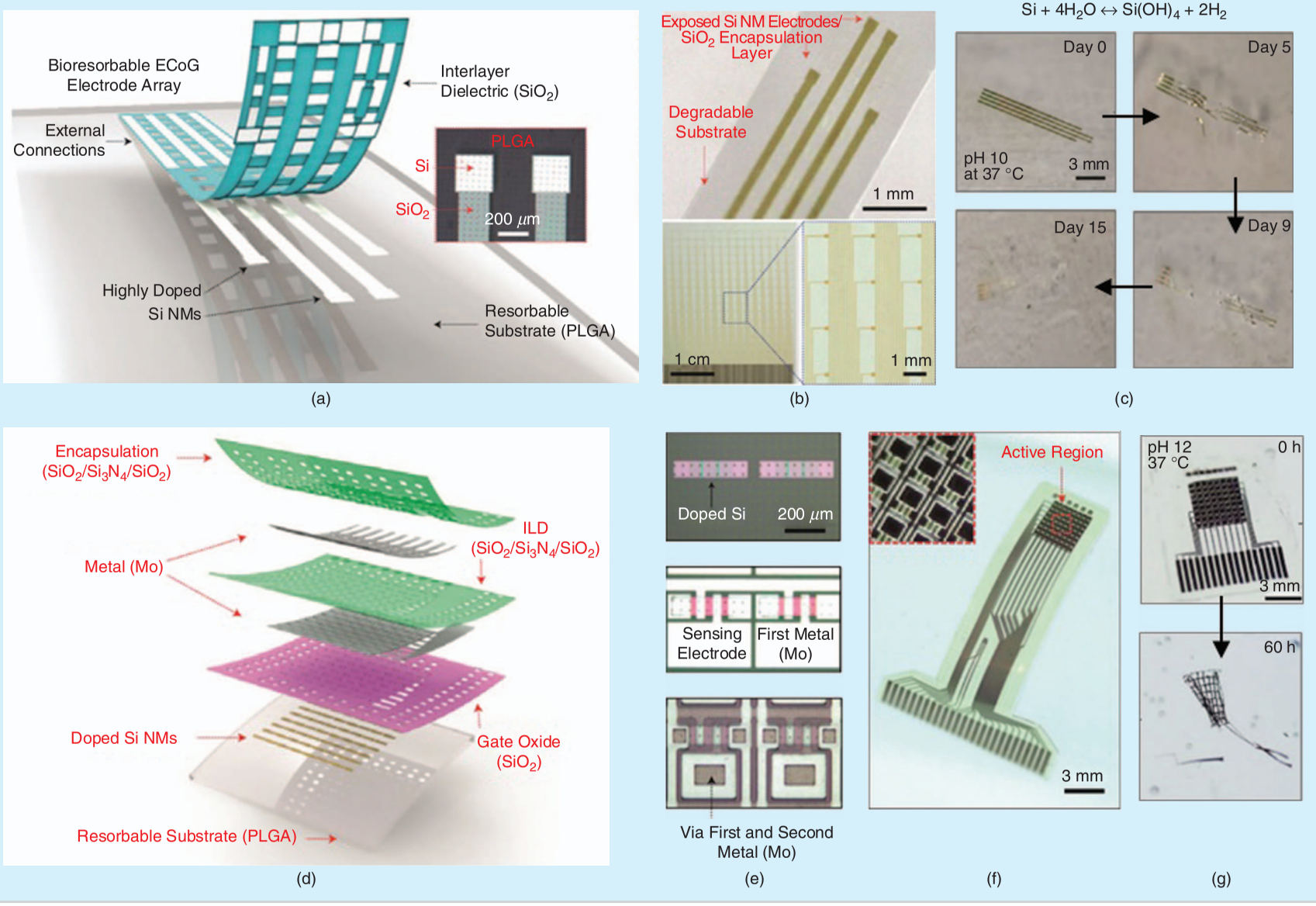

FIGURE 9 Some neural implants have been created using resorbable materials: (a) a typical bioresorbable electrode array, (b) Highly dense electrode array using the similar architecture of all biosorbable materials, (c) a brain implant's resorption process over 15 days, (d) a schematic of a resorbable multiplexed electrode array, (e) fabricated structure of a pair of unit cells from the multiplexed electrode array shown (f) on the complete ultrathin multiplexed device, and (f) a brain implant's active-circuit area and (g) its resorption over 60 h. NM: nanomembrane; PLGA: poly(lactic-co-glycolic acid); Si_3N_4: silicon nitride; Mo: molybdenum [58].

period of time, it must be able to continue performing during the resorption process. Matching this requirement, the Si nanomembrane-based device was eventually resorbed into the brain's biofluid, but before doing so captured action potentials for nearly 30 days. The resorption of Si material needs to be smooth, flake-free, and crack-free over the operational lifetime of the device.

CONCLUSION

In this review, we provided an overview of some of the technology for capturing action-potential signals from the brain. We discussed the recent progress in the area of soft Si membrane-based electrode arrays and their advantages over other existing technology for highly promising advances in BMIs. Although the semi-invasive neural recording method has developed considerably, excellent spatiotemporal resolution for the next generation of μECoG devices still must be engineered. These applications need to implement active-circuit electrode arrays to achieve a high density for precise electrical imaging using ultraconformal, intracranial, implantable devices.

To realize a smooth BMI, the market demands comfortable and mechanically imperceptible brain implants where ultrathin-film engineering and nano/microfabrication techniques play a critical role in developing and processing materials at nanoscale thickness. From a safety perspective, high-resolution electronic imaging using active-circuit architectures is characterized by electrical losses that generate heat, which can cause concern when the resolution improvement follows Moore's law. The heat produced by the neural implants must be critically analyzed and targeted to be minimized, so as not to cause a temperature increase of more than 1°C to preserve long-term brain tissue health. Furthermore, most penetrating devices use injection needles or some sort of stiffer injection methods. These can cause dimples, scars, or tissue infarction during injection and retraction. Thus, engineered solutions need to develop safer modes of injection of penetrating devices.

As reviewed in the previous section, bioresorbability possesses promising advantages for the long-term use of neural implants and for avoiding the critical and costly procedure of surgically removing the implant. The achieved and reported lifetime of Si-based resorbable devices is, so far, limited to nearly 30 days, with the start of performance degradation after two weeks. The decrease in performance obviously decreases the SNR, and, hence, there remain issues to be addressed. Therefore, such bioresorbable devices require well-controlled triggering to initiate their mechanism so the biocompatible resorption process can be manipulated as needed.

The signals that characterize the sulci and grooves are quite strong and could be very useful to study or harness with BMI technology. However, along with the narrow bending radius of these intricate surfaces, the brain grooves also contain blood vessels of various diameters. Thus, together with ultralow bending stiffness, implants require strong surface adhesion and superconformability to all curvilinear surfaces. In terms of performance, neural engineers and scientists also seek high spatiotemporal resolution in mapping a broad range of signals, including low-frequency signals to study the root causes and effects of several neural disorders that generate low-frequency action potentials.

ACKNOWLEDGMENTS

This work is supported by the National Science Foundation (ECCS-1509763 and CMMI-1554499) and the Doctoral New Investigator grant (PRF#56840) from the American Chemical Society Petroleum Research Fund.

ABOUT THE AUTHORS

Anish Thukral (athukral@uh.edu) is with the Department of Mechanical Engineering, University of Houston, Texas.

Faheem Ershad (faheem.ersh@gmail.com) is with the Department of Biomedical Engineering, University of Houston, Texas.

Nada Enan (nadayenan@gmail.com) is with the Department of Biomedical Engineering, University of Houston, Texas.

Zhoulyu Rao (zhoulyur@gmail.com) is with the Materials Science and Engineering Program, University of Houston, Texas.

Cunjiang Yu (cyu15@uh.edu) is with the Department of Mechanical Engineering, Department of Electrical and Computer Engineering, Materials Science and Engineering Program, University of Houston, Texas.

REFERENCES

[1] K. C. Cheung, "Implantable microscale neural interfaces," *Biomed. Microdevices*, vol. 9, pp. 923–938, Dec. 1, 2007.

[2] D. J. McFarland, L. A. Miner, T. M. Vaughan, and J. R. Wolpaw, "Mu and beta rhythm topographies during motor imagery and actual movements," *Brain Topog.*, vol. 12, pp. 177–186, Mar. 1, 2000.

[3] J. L. Collinger, B. Wodlinger, J. E. Downey, W. Wang, E. C. Tyler-Kabara, D. J. Weber, A. J. C. McMorland, M. Velliste, M. L. Boninger, and A. B. Schwartz, "High-performance neuroprosthetic control by an individual with tetraplegia," *Lancet*, vol. 381, pp. 557–564, Dec. 2012.

[4] R. Muller, H. P. Le, W. Li, P. Ledochowitsch, S. Gambini, T. Bjorninen, A. Koralek, J. M. Carmena, M. M. Maharbiz, E. Alon, and J. M. Rabaey, "A minimally invasive 64-channel wireless µECoG implant," *IEEE J. Solid-State Circuits*, vol. 50, pp. 344–359, Nov. 2015.

[5] J. R. Manning, J. Jacobs, I. Fried, and M. J. Kahana, "Broadband shifts in local field potential power spectra are correlated with single-neuron spiking in humans," *J. Neurosci.*, vol. 29, pp. 13,613–13,620, Oct. 2009.

[6] K. J. Miller, L. B. Sorensen, J. G. Ojemann, and M. den Nijs. (2009). Power-law scaling in the brain surface electric potential. *PLoS Computation Biol.* [Online]. 5. Available: https://doi.org/10.1371/journal.pcbi.1000609

[7] K. J. Miller, C. J. Honey, D. Hermes, R. P. N. Rao, M. denNijs, and J. G. Ojemann, "Broadband changes in the cortical surface potential track activation of functionally diverse neuronal populations," *NeuroImage*, vol. 85, pp. 711–720, Jan. 15, 2014.

[8] D. T. Bundy, M. Pahwa, N. Szrama, and E. C. Leuthardt, "Decoding three-dimensional reaching movements using electrocorticographic signals in humans," *J. Neural Eng.*, vol. 13, Apr. 2016.

[9] T. Kaiju, K. Doi, M. Yokota, K. Watanabe, M. Inoue, H. Ando, et al. "High spatiotemporal resolution ECoG recording of somatosensory evoked potentials with flexible micro-electrode arrays," *Frontiers Neural Circuits*, vol. 11, 2017. doi: 10.3389/fncir.2017.00020.

[10] T. Pistohl, T. Ball, A. Schulze-Bonhage, A. Aertsen, and C. Mehring, "Prediction of arm movement trajectories from ECoG-recordings in humans," *J. Neurosci. Methods*, vol. 167, pp. 105–114, Jan. 15, 2008.

[11] S. Morishita, K. Sato, H. Watanabe, Y. Nishimura, T. Isa, R. Kato, T. Nakamura, and H. Yokoi, "Brain-machine interface to control a prosthetic arm with monkey ECoGs during periodic movements," *Frontiers Neurosci.*, vol. 8, Dec. 12, 2014.

[12] P. Brunner, A. L. Ritaccio, J. F. Emrich, H. Bischof, and G. Schalk, "Rapid communication with a 'P300' matrix speller using electrocorticographic signals (ECoG)," *Frontiers Neurosci.*, vol. 5, 2011. doi: 10.3389/fnins.2011.00005.

[13] D. T. Bundy, M. Pahwa, N. Szrama, and E. C. Leuthardt, "Decoding three-dimensional reaching movements using electrocorticographic signals in humans," *J. Neural Eng.*, vol. 13, 2016.

[14] S. I. Park, D. S. Brenner, G. Shin, and C. D. Morgan, "Soft, stretchable, fully implantable miniaturized optoelectronic systems for wireless optogenetics," vol. 33, pp. 1280–1286, Dec. 2015.

[15] R. Chen, A. Canales, and P. Anikeeva, "Neural recording and modulation technologies," *Nature Rev. Mater.*, vol. 2, 2017.

[16] P. Rajasethupathy, E. Ferenczi, and K. Deisseroth, "Targeting neural circuits," *Cell*, vol. 165, no. 3, pp. 524–534, 2016.

[17] T. I. Kim, J. G. McCall, Y. H. Jung, X. Huang, E. R. Siuda, Y. Li, J. Song, Y. M. Song, H. A. Pao, R. H. Kim, C. Lu, S. D. Lee, I. S. Song, G. Shin, R. Al-Hasani, S. Kim, M. P. Tan, Y. Huang, F. G. Omenetto, J. A. Rogers, and M. R. Bruchas, "Injectable, cellular-scale optoelectronics with applications for wireless optogenetics," *Science*, vol. 340, pp. 211–216, Apr. 12 2013.

[18] R.-H. Kim, D.-H. Kim, J. Xiao, B. H. Kim, S.-I. Park, B. Panilaitis, R. Ghaffari, J. Yao, M. Li, Z. Liu, V. Malyarchuk, D. G. Kim, A.-P. Le, R. G. Nuzzo, D. L. Kaplan, F. G. Omenetto, Y. Huang, Z. Kang, and J. A. Rogers, "Waterproof AlInGaP optoelectronics on stretchable substrates with applications in biomedicine and robotics," *Nature Mater.*, vol. 9, pp. 929–937, Oct. 2010.

[19] J. Wang, M. Trumpis, M. Insanally, R. Froemke, and J. Viventi, "A low-cost, multiplexed electrophysiology system for chronic mu ECoG recordings in rodents," in *Proc. 36th Annu. Int. Conf. IEEE Engineering in Medicine and Biology Society*, 2014, pp. 5256–5259.

[20] N. Nakasatp, M. F. Levesque, D. S. Barth, C. Baumgartner, R. L. Rogers, and W. W. Sutherling, "Comparisons of MEG, EEG, and ECoG source localization in neocortical partial epilepsy in humans," *Electroencephalog. Clin. Neurophysiol.*, vol. 91, pp. 171–178, Sept. 1, 1994.

[21] E. L. Air, E. Ryapolova-Webb, C. de Hemptinne, J. L. Ostrem, N. B. Galifianakis, P. S. Larson, E. F. Chang, and P. A. Starr, "Acute effects of thalamic deep brain stimulation and thalamotomy on sensorimotor cortex local field potentials in essential tremor," *Clin. Neurophysiol.: Official J. Int. Fed. Clin. Neurophysiol.*, vol. 123, pp. 2232–2238, May 26, 2012.

[22] D. Khodagholy, J. N. Gelinas, Z. Zhao, M. Yeh, M. Long, J. D. Greenlee, W. Doyle, O. Devinsky, and G. Buzsáki, "Organic electronics for high-resolution electrocorticography of the human brain," *Sci. Advances*, vol. 2, no. 11, 2016. doi: 10.1126/sciadv.1601027.

[23] C. S. Mestais, G. Charvet, F. Sauter-Starace, M. Foerster, D. Ratel, and A. L. Benabid, "WIMAGINE: Wireless 64-channel ECoG recording implant for long term clinical applications," *IEEE Trans. Neural Syst. Rehabil. Eng.*, vol. 23, pp. 10–21, 2015.

[24] F. Panov, E. Levin, C. de Hemptinne, N. C. Swann, S. Qasim, S. Miocinovic, J. L. Ostrem, and P. A. Starr, "Intraoperative electrocorticography for physiological research in movement disorders: Principles and experience in 200 cases," *J. Neurosurg.*, vol. 126, pp. 122–131, Jan. 2017.

[25] "Fostering reproducible fMRI research," *Nature Neurosci.*, vol. 20, no. 3, Feb. 23, 2017. doi: 10.1038/nn.4521.

[26] A. Meyer-Lindenberg, "From maps to mechanisms through neuroimaging of schizophrenia," *Nature*, vol. 468, Nov. 10, 2010. doi: 10.1038/nature09569.

[27] E. Asano, C. Juhász, A. Shah, O. Muzik, D. C. Chugani, J. Shah, S. Sood, and H. T. Chugani, "Origin and propagation of epileptic spasms delineated on electrocorticography," *Epilepsia*, vol. 46, pp. 1086–1097, June 2005.

[28] H. A. C. Wark, R. Sharma, K. S. Mathews, E. Fernandez, J. Yoo, B. Christensen, P. Tresco, L. Rieth, F. Solzbacher, R. A. Normann, and P. Tathireddy, "A new high-density (25 electrodes/mm^2) penetrating microelectrode array for recording and stimulating sub-millimeter neuroanatomical structures," *J. Neural Eng.*, vol. 10, May 2013. doi: 10.1088/1741-2560/10/4/045003.

[29] A. N. Richard and F. Eduardo, "Clinical applications of penetrating neural interfaces and Utah Electrode Array technologies," *J. Neural Eng.*, vol. 13, 2016.

[30] J. Bartels, D. Andreasen, P. Ehirim, H. Mao, S. Seibert, E. J. Wright, and P. Kennedy, "Neurotrophic electrode: Method of assembly and implantation into human motor speech cortex," *J. Neurosci. Methods*, vol. 174, pp. 168–176, July 10, 2008.

[31] J. M. Barnes, L. Przybyla, and V. M. Weaver, "Tissue mechanics regulate brain development, homeostasis and disease," *J. Cell Sci.*, vol. 130, pp. 71–82, 2017.

[32] D. Prodanov and J. Delbeke, "Mechanical and biological interactions of implants with the brain and their impact on implant design," *Frontiers Neurosci.*, vol. 10, 2016.

[33] E. Fernández, B. Greger, P. A. House, I. Aranda, C. Botella, J. Albisua, C. Soto-Sánchez, A. Alfaro, and R. A. Normann, "Acute human brain responses to intracortical microelectrode arrays: Challenges and future prospects," *Frontiers Neuroeng.*, vol. 7, 2014.

[34] R. Green and M. R. Abidian, "Conducting polymers for neural prosthetic and neural interface applications," *Advanced Mater.*, vol. 27, pp. 7620–7637, 2015.

[35] S. Wang, M. Li, J. Wu, D.-H. Kim, N. Lu, Y. Su, Z. Kang, Y. Huang, and J. A. Rogers, "Mechanics of epidermal electronics," *J. Appl. Mech.*, vol. 79, no. 3, 2012. doi: 10.1115/1.4005963.

[36] D.-H. Kim, J. Viventi, J. J. Amsden, J. Xiao, L. Vigeland, Y.-S. Kim, J. A. Blanco, B. Panilaitis, E. S. Frechette, D. Contreras, D. L. Kaplan, F. G. Omenetto, Y. Huang, K.-C. Hwang, M. R. Zakin, B. Litt, and J. A. Rogers, "Dissolvable films of silk fibroin for ultrathin conformal bio-integrated electronics," *Nature Mater.*, vol. 9, pp. 511–517, Apr. 18, 2010.

[37] J. Byun, B. Lee, E. Oh, H. Kim, S. Kim, S. Lee, and Y. Hong, "Fully printable, strain-engineered electronic wrap for customizable soft electronics," *Scientific Rep.*, vol. 7, Mar. 24, 2017. doi:10.1038/srep45328.

[38] J. A. Fan, W.-H. Yeo, Y. Su, Y. Hattori, W. Lee, S.-Y. Jung, Y. Zhang, Z. Liu, H. Cheng, L. Falgout, M. Bajema, T. Coleman, D. Gregoire, R. J. Larsen, Y. Huang, and J. A. Rogers, "Fractal design concepts for stretchable electronics," *Nature Commun.*, vol. 5, Feb. 7, 2014. doi: 10.1038/ncomms4266.

[39] S. Yang, I.-S. Choi, and R. D. Kamien, "Design of super-conformable, foldable materials via fractal cuts and lattice kirigami," *MRS Bull.*, vol. 41, pp. 130–138, 2016.

[40] S. Lee, Y. Inoue, D. Kim, A. Reuveny, K. Kuribara, T. Yokota, J. Reeder, M. Sekino, T. Sekitani, Y. Abe, and T. Someya, "A strain-absorbing design for tissue–machine interfaces using a tunable adhesive gel," *Nature Commun.*, vol. 5, Dec. 19, 2014. doi: 10.1038/ncomms6898.

[41] X. Wang, C. A. Gkogkidis, O. Iljina, L. D. J. Fiederer, C. Henle, I. Mader, J. Kaminsky, T. Stieglitz, M. Gierthmuehlen, and T. Ball, "Mapping the fine structure of cortical activity with different micro-ECoG electrode array geometries," *J. Neural Eng.*, vol. 14, 2017.

[42] P. T. Wang, C. E. King, C. M. McCrimmon, J. J. Lin, M. Sazgar, F. P. Hsu, S. J. Shaw, D. E. Millet, L. A. Chui, C. Y. Liu, A. H. Do, and Z. Nenadic, "Comparison of decoding resolution of standard and high-density electrocorticogram electrodes," *J. Neural Eng.*, vol. 13, 2016.

[43] M. W. Slutzky, L. R. Jordan, T. Krieg, M. Chen, D. J. Mogul, and L. E. Miller, "Optimal spacing of surface electrode arrays for brain–machine interface applications," *J. Neural Eng.*, vol. 7, 2010.

[44] B. Wodlinger, A. D. Degenhart, J. L. Collinger, E. C. Tyler-Kabara, and W. Wang, "The impact of electrode characteristics on electrocorticography (ECoG)," in *Proc. Annu. Int. Conf. IEEE Engineering in Medicine and Biology Society*, 2011, pp. 3083–3086.

[45] W. Wang, A. D. Degenhart, J. L. Collinger, R. Vinjamuri, G. P. Sudre, P. D. Adelson, D. L. Holder, E. C. Leuthardt, D. W. Moran, M. L. Boninger, A. B. Schwartz, D. J. Crammond, E. C. Tyler-Kabara, and D. J. Weber, "Human motor cortical activity recorded with micro-ECoG electrodes, during individual finger movements," in *Proc. Annu. Int. Conf. IEEE Engineering in Medicine and Biology Society*, 2009, pp. 586–589.

[46] L. Muller, L. S. Hamilton, E. Edwards, K. E. Bouchard, and E. F. Chang, "Spatial resolution dependence on spectral frequency in human speech cortex electrocorticography," *J. Neural Eng.*, vol. 13, Aug. 31, 2016. doi: 10.1088/1741-2560/13/5/056013.

[47] R. Birthe, B. Conrado, O. Robert, F. Pascal, and S. Thomas, "A MEMS-based flexible multichannel ECoG-electrode array," *J. Neural Eng.*, vol. 6, 2009.

[48] Z. Xiang, J. Liu, and C. Lee, "A flexible three-dimensional electrode mesh: An enabling technology for wireless brain–computer interface prostheses," *Microsyst. Nanoeng.*, vol. 2, May 23, 2016. doi: 10.1038/micronano.2016.12.

[49] W. Shen, L. Karumbaiah, X. Liu, T. Saxena, S. Chen, R. Patkar, R. V. Bellamkonda, and M. G. Allen, "Extracellular matrix-based intracortical microelectrodes: Toward a microfabricated neural interface based on natural materials," *Microsyst. Nanoeng.*, vol. 1, June 29, 2015. doi: 10.1038/micronano.2015.10.

[50] L. Luan, X. Wei, Z. Zhao, J. J. Siegel, O. Potnis, C. A. Tuppen, S. Lin, S. Kazmi, R. A. Fowler, S. Holloway, A. K. Dunn, R. A. Chitwood, and C. Xie, "Ultraflexible nanoelectronic probes form reliable, glial scar–free neural integration," *Sci. Advances*, vol. 3, no. 2, 2017. doi: 10.1126/sciadv.1601966.

[51] C. Xie, J. Liu, T.-M. Fu, X. Dai, W. Zhou, and C. M. Lieber, "Three-dimensional macroporous nanoelectronic networks as minimally invasive brain probes," *Nature Mater.*, vol. 14, pp. 1286–1292, Oct. 5, 2015.

[52] K. A. Ng, E. Greenwald, Y. P. Xu, and N. V. Thakor, "Implantable neurotechnologies: A review of integrated circuit neural amplifiers," *Med. Biolog. Eng. Comput.*, vol. 54, pp. 45–62, Jan. 22, 2016.

[53] P. Ruther and O. Paul, "New approaches for CMOS-based devices for large-scale neural recording," *Current Opinion Neurobiol.*, vol. 32, pp. 31–37, June 1, 2015.

[54] J. Viventi, D.-H. Kim, L. Vigeland, E. S. Frechette, J. A. Blanco, Y.-S. Kim, A. E. Avrin, V. R. Tiruvadi, S.-W. Hwang, A. C. Vanleer, D. F. Wulsin, K. Davis, C. E. Gelber, L. Palmer, J. V. d. Spiegel, J. Wu, J. Xiao, Y. Huang, D. Contreras, J. A. Rogers, and B. Litt, "Flexible, foldable, actively multiplexed, high-density electrode array for mapping brain activity in vivo," *Nature Neurosci.*, vol. 14, pp. 1599–1605, Nov. 13, 2011.

[55] J. Abbott, T. Ye, L. Qin, M. Jorgolli, R. S. Gertner, D. Ham, and H. Park, "CMOS nanoelectrode array for all-electrical intracellular electrophysiological imaging," *Nature Nanotechnol.*, vol. 12, pp. 460–466, Feb. 13, 2017.

[56] W. Lee, D. Kim, N. Matsuhisa, M. Nagase, M. Sekino, G. G. Malliaras, T. Yokota, and T. Someya, "Transparent, conformable, active multielectrode array using organic electrochemical transistors," *Proc. Nat. Acad. Sci.*, vol. 114, pp. 10,554–10,559, Oct. 3, 2017.

[57] P. M. Sberna, M. Trifunovic, and R. Ishihara, "Solution-based fabrication of polycrystalline Si thin-film transistors from recycled polysilanes," *ACS Sustainable Chem. Eng.*, vol. 5, pp. 5642–5645, July 3, 2017.

[58] K. J. Yu, D. Kuzum, S.-W. Hwang, B. H. Kim, H. Juul, N. H. Kim, et al., "Bioresorbable silicon electronics for transient spatiotemporal mapping of electrical activity from the cerebral cortex," *Nature Mater.*, vol. 15, pp. 782–791, Apr. 2016.

[59] K. Sim, Z. Rao, D. Yang, Y. Li, and C. Yu, "Curvy Surface Conformal Ultra-Thin Transfer Printed Si Optoelectronic Penetrating Microprobe Arrays," NPJ Flexible Electronics. doi: 10.1038/s41528-017-0015-8.

N